Anharmonic Decay of Coherent Optical Phonons in Antimony

doi: 10.7566/JPSJ.84.024708

Anharmonic Decay of Coherent Optical Phonons in Antimony

Muneaki Hase[1,2*], Kiminori Ushida[3], and Masahiro Kitajima[1,2,4]

[1]*Division of Applied Physics, Faculty of Pure and Applied Sciences, University of Tsukuba, Tsukuba 305-8573, Japan*
[2]*National Institute for Materials Science, Tsukuba 305-0047, Japan*
[3]*Department of Chemistry, School of Science, Kitasato University, Sagamihara, Kanagawa 252-0373, Japan*
[4]*LxRay Co., Ltd. Nishinomiya 663-8172, Japan*

(Received December 5, 2014)

The anharmonic decay of coherent optical phonons in the semimetal Sb has been investigated by a femtosecond pump-probe technique. The coherent A_{1g} mode is observed in the time domain in a wide temperature range of 7 – 290 K. The decay rate (the inverse of the dephasing time) systematically increases as the lattice temperature increases, which is well explained by anharmonic phonon-phonon coupling, causing the decay of the optical phonon into two acoustic phonon modes. The frequency of the A_{1g} mode decreases with increasing temperature, which is interpreted as the results of both thermal expansion and anharmonic phonon-phonon coupling. The temperature dependence of the amplitude of the coherent A_{1g} mode exhibits a decrease with increasing lattice temperature, which is well reproduced by considering the peak intensity of spontaneous Raman scattering assuming a Lorentzian line shape with the linewidth controlled by the anharmonic decay, and this model is applicable to other metallic systems, such as Zn.

1. Introduction

In recent years, coherent phonons have been studied by using a femtosecond pump-probe technique in various material systems, including semiconductors,[1,2] metals,[3,4] superconductors,[5–7] organic conductors,[8] and phase-change materials.[9,10] The coherent phonons can be generated by ultrashort laser pulses with a high degree of temporal coherence. The nature of the coherent phonons has been extensively studied in semimetals[11] and semiconductors,[12] where the main focus was the generation mechanism. Because the coherent phonons are lattice vibrations having the same phase in time, the dephasing of the coherent phonons is directly monitored by optical pump-probe measurements.

Studies on the dephasing process are particularly important for understanding the nature of in-phase coherent phonons. The dephasing of coherent phonons excited by picosecond pulses has been examined using time-resolved coherent anti-Stokes Raman scattering (CARS).[13,14] The phonon decay rate can be generally described as the sum of the anharmonic decay rate and the pure dephasing rate.[15] The main channels for the relaxation of incoherent optical phonons in semiconductors are considered to be the dephasing originating from the phonon-phonon interaction caused by the anharmonicity of the lattice potential. In this channel, the excited optical phonons decay into acoustic phonons.[16,17] A direct comparison has been made between the results obtained by time-resolved CARS and Raman scattering spectroscopies.[14,15] The anharmonic phonon decay of coherent phonons was first confirmed by Hase *et al.* in Bi by measuring the temperature dependence of the dephasing time or decay rate (the inverse of the dephasing time).[18] It has also been shown that the dephasing of the coherent optical phonon is very sensitive to the density of lattice defects (vacancies).[19,20] However, systematic studies of the dephasing of coherent optical phonons in semimetals other than Bi excited by femtosecond laser pulses are still few.

In this paper, the dephasing process of coherent optical phonons in the semimetal antimony (Sb) is studied by femtosecond pump-probe reflectivity measurements in the temperature range from 7 to 290 K. The amplitude, dephasing time, and frequency of the coherent optical phonons have been precisely measured. The decay rate and frequency show systematic changes as functions of the lattice temperature, similar to those in Bi, and are reproduced by a model based on anharmonic lattice effects. The amplitude of the coherent phonon also exhibits a systematic decrease with increasing lattice temperature, which is well fit using the model based on the phonon occupation number proposed by Misochko *et al.*[21]

2. Experimental Technique

The sample used in this study was a single crystal of Sb with the (0001) surface. The femtosecond pump-probe measurements were carried out in the temperature range from ≈7 to 290 K using a closed-cycle cryostat. The light source used was a mode-locked Ti:sapphire laser with a central wavelength of 800 nm, providing ≈20 fs pulses at a repetition rate of 87 MHz. The pump and probe beams were polarized orthogonal to each other to avoid a scattered pump beam. Both pump and probe beams were focused onto a diameter of ≈100 μm on the sample. The average powers of the pump and probe beams were fixed at 120 and 5 mW, respectively, from which we estimated the pump fluence to be 18.4 μJ/cm^2 at 120 mW. By changing the optical path length of the probe beam, the reflectivity change ($\Delta R/R$) was recorded as a function of the delay time. This isotropic reflectivity measurement enables us to predominantly detect the fully symmetric A_{1g} mode in Sb, while the nonsymmetric E_g mode is generally masked.[3] Thus, the determination of the phonon parameters, i.e., amplitude, dephasing time, and frequency, is accurate in the present study because a single damped harmonic oscillator model can fit the coherent phonon signal with the smallest number of parameters.[18]

*E-mail: mhase@bk.tsukuba.ac.jp

3. Experimental Results and Analysis

Figure 1 shows the transient reflectivity change ($\Delta R/R$) recorded in an Sb single crystal at lattice temperatures of between 7 and 290 K. The coherent oscillation of the fully symmetric A_{1g} mode (≈ 150 cm^{-1} = 4.52 THz at 290 K),[3,22] superimposed on the photoexcited carrier background, is observed in this wide temperature range. As the temperature is decreased, the dephasing time becomes longer and the amplitude of the coherent A_{1g} mode increases. In this study the frequency, amplitude, and dephasing time of the coherent A_{1g} mode at various temperatures were determined by fitting the time-domain data to a damped harmonic oscillation with an exponential decay function:[18]

$$\frac{\Delta R(t)}{R} = A\exp\left(-\frac{t}{\tau}\right)\cos(\omega_{A_{1g}}t+\phi)+B\left[\exp\left(-\frac{t}{\tau_1}\right)-\exp\left(-\frac{t}{\tau_2}\right)\right], \quad (1)$$

where A is the amplitude, $\omega_{A_{1g}}$ is the frequency, τ is the dephasing time, and ϕ is the initial phase of the coherent A_{1g} mode. The second term arises from the photoexcited carriers. Here, B is the amplitude, and τ_1 and τ_2 are the relaxation time and rising time of the electric component, respectively. The fitting results in Fig. 1 are satisfactory and thus we obtain the phonon parameters. The initial phase (ϕ) obtained is nearly zero, indicating that the coherent oscillation is cosine-like. This phase value matches with the previous results on Sb, that is, the generation mechanism of the coherent A_{1g} mode is governed by the displacive excitation of the coherent phonon (DECP) model[3,23] or Raman scattering finite lifetime (RSFL) model,[22,24] the latter of which takes both the finite lifetime of the coupled charge carrier density (a characteristic nature of DECP) and the stimulated Raman scattering into account. The amplitude of the electric component, B, exhibits increase by $\sim 15\%$ as the temperature is lowered as seen in Fig. 1, suggesting that the photoexcited carrier density increases with decreasing lattice temperature.[4] We will discuss the temperature dependence of the parameter B together with the amplitude of the coherent A_{1g} mode (A) later. The values of the relaxation times τ_1 and τ_2 do not systematically change with the temperature, and therefore we will not discuss the time constants of the electric component in detail in the present paper. Hereafter, the temperature dependences of the decay rate, frequency, and amplitude of the coherent optical phonons are mainly focused on and explored.

In Fig. 2, the decay rate (the inverse of the dephasing time) of the A_{1g} mode at different temperatures obtained by time-domain measurement is plotted. The frequency of the coherent A_{1g} mode is also plotted in the inset. It shifts from 4.67 to 4.52 THz when the temperature increases from 7 to 290 K. The decay rate of the A_{1g} mode monotonically increases as the lattice temperature rises, which is comparable to the results for Bi films.[18] Because of this behavior, we attempted to fit our results using an anharmonic decay model,[17] in which the optical phonon decays into two acoustic phonons with half the frequency of the optical mode ($\omega_{A_{1g}}/2$) and with opposite wavevectors,[4,17,18,25]

$$\Gamma_{A_{1g}} = \Gamma_0 + \Gamma(1 + 2n_{A_{1g}/2}), \quad (2)$$

where Γ_0 is the background contribution due to impurity and defect scattering, Γ is the anharmonic coefficient, $n_{A_{1g}/2} = [\exp(\hbar\omega_{A_{1g}}/2k_BT)-1]^{-1}$ is the Bose-Einstein factor, and k_B is the Boltzmann constant. The fitting of the time-domain data to Eq. (2) is shown in Fig. 2, where we obtain $\Gamma_0 = 0.1$ ps^{-1} and $\Gamma = 0.06$ ps^{-1} for Sb. Thus, the temperature dependence of the decay rate of the coherent A_{1g} mode is well described using Eq. (2), indicating that the dephasing of the coherent A_{1g} mode is governed by the anharmonic phonon-phonon coupling. In the same manner, the frequency softening of the A_{1g} mode is expressed by taking into account the contributions from the thermal expansion and anharmonic coupling, both of which are related to the cubic anharmonic term,[25,26]

$$\omega_{A_{1g}} = \omega_0 + \Delta_0(T) + \Omega(1 + 2n_{A_{1g}/2}), \quad (3)$$

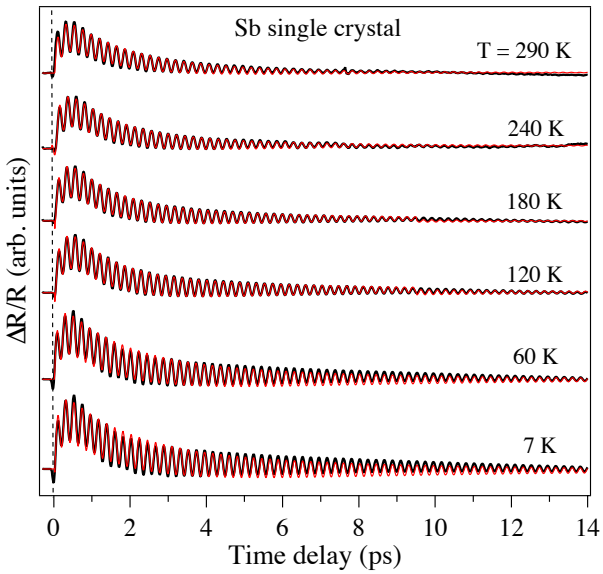

Fig. 1. (Color) Time-resolved reflectivity changes for Sb single crystal at temperatures between 7 and 290 K. The black thin lines are the data, while the red lines are the fit with Eq. (1).

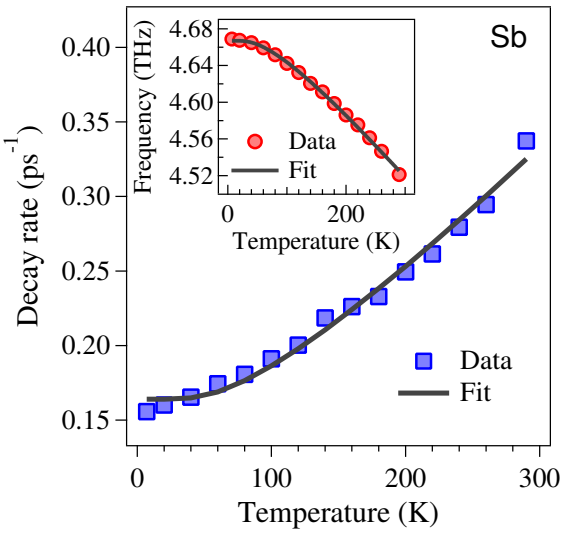

Fig. 2. (Color online) Decay rate of the A_{1g} mode together with frequency (inset) as a function of lattice temperature. The solid line represents the fit to the data using Eq. (2) with $\Gamma_0 = 0.1$ ps^{-1} and $\Gamma = 0.06$ ps^{-1}. In the inset, the frequency of the A_{1g} mode is fit to the model given by Eqs. (3) and (4), which is represented by the solid line.

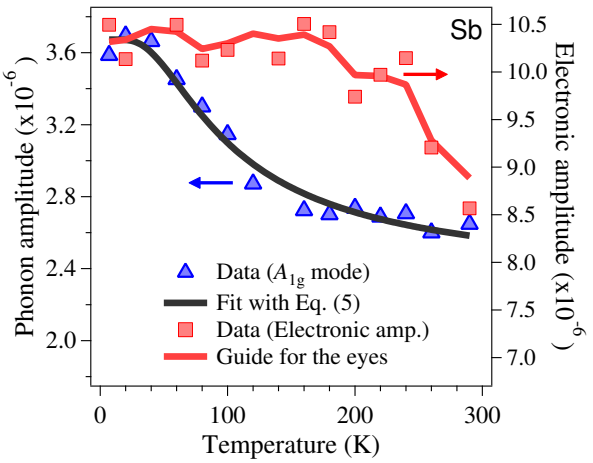

Fig. 3. (Color online) Amplitudes of the coherent A_{1g} mode (A) and electronic component (B) as functions of lattice temperature. The black solid curve represents the fit to the data using Eq. (5), using a fitting parameter of $A_0 = 1.8\times10^{-6}$ and a temperature-independent background of 1.9×10^{-6}. The red solid line is a guide for the eyes.

where ω_0 is the harmonic frequency at the lowest temperature limit, Ω is an anharmonic constant, and $\Delta_0(T)$ represents the frequency shift due to the thermal expansion of the lattice, which is given by[26)]

$$\Delta_0(T) = -\omega_0\gamma\int_0^T [\alpha_{//}(T') + 2\alpha_{\perp}(T')]dT', \qquad (4)$$

where γ is the Grüneisen parameter, and $\alpha_{//}(T')$ and $\alpha_{\perp}(T')$ are the linear thermal expansion coefficients along directions parallel and perpendicular to the c-axis, respectively. To calculate $\Delta_0(T)$, we took the experimental linear thermal expansion coefficients and the Grüneisen parameter (γ = 1) measured by White,[27)] and thus model fitting based on Eqs. (3) and (4) was carried out. The fitting result of the time-domain data to Eqs. (3) and (4) is shown in the inset of Fig. 2, where we obtain ω_0 = 4.75 THz and Ω = - 0.087 THz, the latter of which is comparable to the result (Ω = - 0.056 THz) for Bi films.[18)] It should be noted here that the contribution from the thermal expansion to the frequency softening becomes effective at $T \geq$ 100 K because the linear thermal expansion coefficients are rather small at $T \leq$ 100 K, while they become larger and nearly constant at $T \geq$ 100 K.[27)]

As shown in Fig. 3, the amplitude of the coherent A_{1g} mode increases with decreasing temperature. The ratio of the amplitude of the coherent A_{1g} mode obtained at 7 K to that obtained at 290 K is ≈1.3. A similar temperature dependence of the coherent phonon amplitude was observed for the E_g mode in a single crystal of Sb by Ishioka *et al.*, while they observed rather flat behavior for the A_{1g} mode.[22)] The difference in the amplitude of the coherent A_{1g} mode between the two measurements might partly originate from the different temperature dependence of the electric component, since the amplitude of the A_{1g} mode is proportional to the photoexcited carrier density, $A = \kappa B$, where κ is an electron-phonon coupling constant, under the DECP model.[23)] In fact, Ishioka *et al.* observed an increase in the electronic transient between 100 and 200 K by isotropic reflectivity measurements,[22)] while we observed a decrease in the electric component with increasing temperature by the same measurements (see Fig. 3), as was also observed in simple metals.[4)] We fitted the temperature data of the phonon amplitude in Fig. 3 to the expected temperature dependence of the peak intensity of spontaneous Raman scattering assuming a Lorentzian line shape with the linewidth controlled by anharmonic decay.[21)] By using the well-known property of a Lorentzian, the temperature dependence of the peak intensity of the Raman-active A_{1g} mode is proportional to[21,28)]

$$A = A_0\frac{n_{A_{1g}} + 1}{2n_{A_{1g}/2} + 1}, \qquad (5)$$

where A_0 is a constant, $n_{A_{1g}} = [\exp(\hbar\omega_{A_{1g}}/k_BT) - 1]^{-1}$ is the Bose-Einstein factor, and the denominator of Eq. (5) represents the linewidth controlled by the anharmonic decay [see Eq. (2)]. The agreement between the experimental data and the Raman cross section, as shown in Fig. 3, is very good for the temperature range of 7 K $\leq T \leq$ 290 K. The good agreement of the experimental phonon amplitude with Eq. (5) found in Fig. 3 suggests that the RSFL mechanism is predominant in the generation of the coherent A_{1g} mode over the DECP mechanism. This interpretation is further supported by the fact that the temperature dependence of the electronic amplitude (B) exhibits a significantly different nature from that of the coherent A_{1g} mode (A), as shown in Fig. 3, and consequently, the DECP model ($A = \kappa B$) cannot solely account for the observed results.

4. Discussion

Note that in the case of the coherent phonons of bismuth, the E_g mode was also observed at low temperatures even with the isotropic detection scheme.[29)] The intensity of the E_g mode was ≈1/10 of the A_{1g} mode in the Fourier-transformed (FT) spectra. In Sb, there seems to be no E_g component at 7 K in Fig. 1, which was also confirmed by the FT spectra (not shown). A possible reason for the difference in the appearance of the E_g mode between these two different atoms is the polarization dependence of the Raman tensor for the E_g mode. To observe the E_g mode by isotropic detection, one would need to use a highly oriented single-crystal sample and to precisely rotate the pump polarization in the $x - y$ plane to match the appropriate crystal axis,[29)] although a study of the pump-polarization dependence of the E_g mode using such a highly oriented single crystal is beyond the scope of this paper.

Hereafter, we focus on the temperature dependence of the amplitude of the coherent phonon, referring to other metallic systems, since it will give a new insight into the physics of coherent phonons in a wide range of materials. A strong temperature dependence of the coherent optical phonon was observed in the simple metal Zn, in which the temperature dependence was examined in terms of the quasiparticle density.[4)] Figure 4 shows a comparison of the fitting models for the temperature dependence of the amplitude of the coherent optical phonon observed in Zn.[4)]

It is found that the current model, Eq. (5) in the present study, describes the overall data in Fig. 4 reasonably well, although the previous model based on the density of the quasiparticles could also fit the data at $T \geq$ 80 K, while some deviation was found at temperatures lower than 80 K.[4)] Consequently, we conclude that the overall behavior of the coherent phonon amplitude as a function of the lattice temperature is

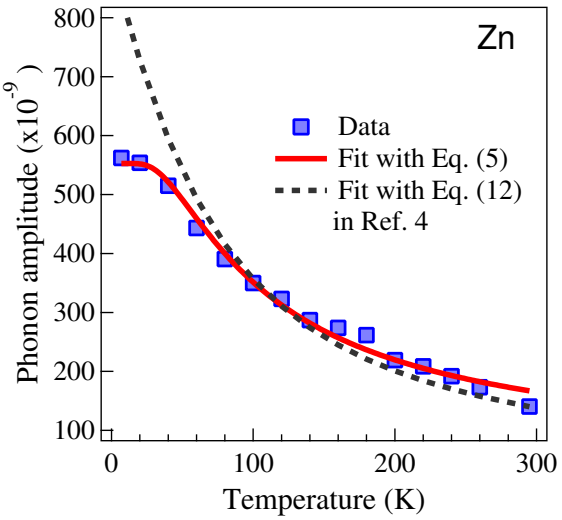

Fig. 4. (Color online) Amplitude of the coherent E_g mode in Zn as a function of lattice temperature (the data were reproduced from Ref. 4). The red solid line represents the fit to the data using Eq. (5), while the dashed line is the fit with Eq. (12) in Ref. 4.

well modeled by Eq. (5) in a wide range of metallic systems (Bi, Sb, and Zn) or in the wide range of the Debye temperature, $\Theta_D \approx 120$ K for Bi, $\Theta_D \approx 210$ K for Sb and $\Theta_D \approx 330$ K for Zn.[30] Note that a plausible reason why the deviation was observed at $T \leq 80$ K for Zn in Fig. 4 between the model in Ref. 4 and the data is the classical nature of the simple model in Ref. 4, in which $A \propto T_e' - T_e$, where T_e' and T_e are the final and initial electron temperatures, respectively. On the contrary, the current model, Eq. (5), is based on the quantum effect described by the Bose-Einstein factor.

5. Conclusion

In conclusion, the temperature dependence of the dynamics of coherent optical phonons in an Sb single crystal has been studied by a femtosecond pump-probe technique at various lattice temperatures. The agreement of the decay rate and the frequency of the coherent A_{1g} mode with the anharmonic model indicates that the dephasing of coherent phonons in antimony is dominated by anharmonic decay (energy relaxation), and that the frequency softening is due to the cubic term of the anharmonicity, in which thermal expansion and anharmonic phonon-phonon coupling play important roles. The coherent phonon amplitude of the A_{1g} mode decreases with the lattice temperature, which is well modeled by the use of the peak intensity of spontaneous Raman scattering and which also satisfactory reproduces the amplitude of the coherent E_g mode in Zn. Thus, in a wide range of metallic systems, the anharmonic lattice effect dominates the temperature dependence of the decay rate, the frequency, and the amplitude of the photoexcited coherent optical phonons.

This work was supported in part by a Grant-in-Aid for Scientific Research from the Ministry of Education, Culture, Sports, Science and Technology of Japan under grant no. KAKENHI-15740188.

1) G. C. Cho, W. Kütt, and H. Kurz, Phys. Rev. Lett. **65**, 764 (1990).
2) K. J. Yee, K. G. Lee, E. Oh, D. S. Kim, and Y. S. Lim, Phys. Rev. Lett. **88**, 105501 (2002).
3) T. K. Cheng, S. D. Bronson, A. S. Kazeroonian, J. S. Moodera, G. Dresselhaus, M. S. Dresselhaus, and E. P. Ippen, Appl. Phys. Lett. **57**, 1004 (1990).
4) M. Hase, K. Ishioka, J. Demsar, K. Ushida, and M. Kitajima, Phys. Rev. B **71**, 184301 (2005).
5) O. V. Misochko, K. Kisoda, K. Sakai, and S. Nakashima, Phys. Rev. B **61**, 4305 (2000).
6) H. Takahashi, Y. Kamihara, H. Koguchi, T. Atou, H. Hosono, I. Katayama, J. Takeda, M. Kitajima, and K. G. Nakamura, J. Phys. Soc. Jpn. **80**, 013707 (2011).
7) K. W. Kim, A. Pashkin, H. Schäfe, M. Beyer, M. Porer, T. Wolf, C. Bernhard, J. Demsar, R. Huber, and A. Leitenstorfer, Nat. Mater. **11**, 497 (2012).
8) K. Onda, S. Ogihara, K. Yonemitsu, N. Maeshima, T. Ishikawa, Y. Okimoto, X. Shao, Y. Nakano, H. Yamochi, G. Saito, and S. Koshihara, Phys. Rev. Lett. **101**, 067403 (2008).
9) M. Först, T. Dekorsy, C. Trappe, M. Laurenzis, H. Kurz, and B. Béchevet, Appl. Phys. Lett. **77**, 1964 (2000).
10) M. Hase, Y. Miyamoto, and J. Tominaga, Phys. Rev. B. **79**, 174112 (2009).
11) G. A. Garrett, T. F. Albrecht, J. F. Whitaker, and R. Merlin, Phys. Rev. Lett. **77**, 3661 (1996).
12) W. A. Kütt, W. Albrecht, and H. Kurz, IEEE J. Quantum Electronics **28**, 2434 (1992).
13) D. von der Linde, J. Kuhl, and H. Klingenberg, Phys. Rev. Lett. **44**, 1505 (1980).
14) W. E. Bron, J. Kuhl, and B. K. Rhee, Phys. Rev. B **34**, 6961 (1986).
15) A. Laubereau and W. Kaiser, Rev. Mod. Phys. **50**, 607 (1978).
16) J. Menendez and M. Cardona, Phys. Rev. B **29**, 2051 (1984).
17) P. G. Klemens, Phys. Rev. **148**, 845 (1966).
18) M. Hase, K. Mizoguchi, H. Harima, S. Nakashima, and K. Sakai, Phys. Rev. B **58**, 5448 (1998).
19) M. Hase, K. Ishioka, M. Kitajima, K. Ushida, and S. Hishita, Appl. Phys. Lett. **76**, 1258 (2000).
20) M. Hase and M. Kitajima, J. Phys.: Condens. Matter **22**, 073201 (2010).
21) O. V. Misochko, K. Ishioka, M. Hase, and M. Kitajima, J. Phys.: Condens. Matter **18**, 10571 (2006).
22) K. Ishioka, M. Kitajima, and O. V. Misochko, J. Appl. Phys. **103**, 123505 (2008).
23) H. J. Zeiger, J. Vidal, T. K. Cheng, E. P. Ippen, G. Dresselhaus, and M. S. Dresselhaus, Phys. Rev. B **45**, 768 (1992).
24) D. M. Riffe and A. J. Sabbah, Phys. Rev. B **76**, 085207 (2007).
25) M. Balkanski, R. F. Wallis, and E. Haro, Phys. Rev. B **28**, 1928 (1983).
26) R. Cuscó, E. Alarcón-Lladó, J. Ibáñez, L. Artús, J. Jiménez, B. Wang, and M. J. Callahan, Phys. Rev. B **75**, 165202 (2007).
27) G. K. White, J. Phys. C: Solid State Phys. **5**, 2731 (1972).
28) N. Kamaraju, S. Kumar, M. Anija, and A. K. Sood, Phys. Rev. B **82**, 195202 (2010).
29) K. Ishioka, M. Kitajima, and O. V. Misochko, J. Appl. Phys. **100**, 093501 (2006).
30) C. Kittel, *Introduction to Solid State Physics* (Wiley, New York, 1986) 6th ed.